A.V. NAZARENKO,[1] V. BLAVATSKA [2]

[1] Bogolyubov Institute for Theoretical Physics, Nat. Acad. of Sci. of Ukraine
(4-b, Metrologichna Str., Kyiv 03680, Ukraine; e-mail: nazarenko@bitp.kiev.ua)
[2] Institute for Condensed Matter Physics, Nat. Acad. of Sci. of Ukraine
(1, Svientsitski Str., Lviv 79011, Ukraine; e-mail: viktoria@icmp.lviv.ua)

UDC 538.93

ASYMMETRIC RANDOM WALK IN A ONE-DIMENSIONAL MULTIZONE ENVIRONMENT

We consider a random walk model in a one-dimensional environment formed by several zones of finite widths with fixed transition probabilities. It is assumed that the transitions to the left and right neighboring points have unequal probabilities. In the continuous limit, we derive analytically the probability distribution function, which is mainly determined by a walker diffusion and a drift and takes perturbatively the interface effects between zones into account. It is used for computing the probability to find a walker at a given space-time point and the time dependence of the mean squared displacement of a walker trajectory, which reveals the transient anomalous diffusion. To justify our approach, the probability function is compared with the results of numerical simulations for the case of three-zone environment.

K e y w o r d s: random walk, inhomogeneous environment, diffusion, advection.

1. Introduction

The present paper is devoted to a deeper study of a random walk (RW) in a one-dimensional inhomogeneous environment consisting of N zones with constant parameters. The base model was formulated in our previous work [1], where we referred to a number of problems [2–9] investigated before and influenced our motivation. In the mentioned work, we applied the analytical approach to find the probability distribution function (PDF) of a walker in a heterogeneous environment.

Here, we supply the RW model by placing an attractor/repulsor at the root point, which serves as a source of the external field (it could be a uniform electric field for a charged walker). Its presence determines the preferable directions of a walk and leads, therefore, to the emergence of an inequality (asymmetry) between the probabilities of transitions to the left and to the right.

Our investigations are stimulated by the application of RW models in many fields such as polymer physics, economics, computer sciences, *etc.* [10]. RW is often considered as a simple mathematical formulation of the diffusion process. The model of random walk is widely used in biophysics and medicine [11,12]. In particular, it is applied to describe the processes of migration and proliferation of a population of cells [13–16].

Moreover, the RW in inhomogeneous environments is of great interest because of its connection with transport phenomena in fractured and porous rocks, diffusion of particles in gels, colloidal solutions, and biological cells (see, e.g., [17] for a review).

Here, we consider the model in a one-dimensional N-zone environment located along a coordinate axis and symmetric under the coordinate sign inversion. The transition probability is assumed to vary within the different zones and to be unequal for the left and right steps. Numerous previous studies dealing with the one-dimensional RW in environments with "inhomogeneities" such as walls [3, 4, 6], stack of permeable barriers [5, 7, 8], or finite-sized barriers [2, 9] revealed the physically significant effects and the non-trivial behavior with pronounced deviations away from the Brownian one. In particular, the time-dependent (transient) diffusion coefficients are observed in an inhomogeneous system of parallel walls with arbitrary permeabilities [5].

The model under consideration is engaged to describe, e.g., the linear chaotic structures passing through a finite number of zones with viscous properties in an external field. Imagining a few-dimensional problem, for a moment, these may be polymer chains crossing the cellular membranes [18]. The model can

be also applied to describe the dynamics of particles in a system with barriers, which are associated with different sorts of the matter or geometry of space. Our goal is to derive an analytical expression for the probability to find a particle as a function of the space-time with regard for the transitions between zones due to the diffusion and advection.

We are interested in catching the new effects caused by a transition probability asymmetry in comparison with the symmetric case [1]. Analytically, we aim to reduce the problem in the continuous limit to finding the PDF from a differential equation with the diffusion coefficient and the drift velocity, which inherit the established step-like space dependence. Further, the space-time evolution might be characterized by the averages, which are found by means of the PDF and allow us to compare the properties of similar models with different parameters. We would like also to demonstrate a strong dependence of the meaningful quantities on the attractive or repulsive character of the starting point. In particular, we will predict the existence of a steady state, when the diffusion and the advection are equilibrated.

As was already shown for the symmetric RW [1], there is a possibility to compare the derived probability function to find a walker at a given point of space-time with the data of numerical simulations. This comparison is performed also in the present study.

From the technical point of view, the time dependence of the mean squared displacement of the RW trajectories in the considered heterogeneous environment is not easily computable. Then we neglect the interface effects, but account accurately for the bulk ones. This simplification is justified previously, where the advection (drift) is absent [1]. There, the time asymptotics of the variance corresponds to a uniform model, while the multizone structure of the environment leads to the emergence of a transient anomalous diffusion at a finite time. These phenomena are investigated here in the drift presence.

The layout of the paper is as follows. In the next section, we fix the random walk rules and obtain the differential equation for a PDF. An approximate PDF is found in Section 3. The probability function is calculated analytically in Section 4 and is compared with the numerical simulations performed. After computing the mean squared displacement in Section 5, we end up with giving the discussion and outlook.

2. Asymmetric RW in N-Zone Environment

We start with a lattice model of RW considered as a Markov process with either a zeroth or unitary step in space after a successive unitary step in time. The walk is determined here by the stationary transition probability $T(x_{t+1}, x_t)$ defined as

$$T(x,y) = p(y)\delta_{x-y,-1} + q(y)\delta_{x-y,1} + r(y)\delta_{x-y,0}, \quad (1)$$

where $\sum_{x\in\mathbb{Z}} T(x,y) = p(y)+q(y)+r(y) = 1$ is implied for a fixed $y \in \mathbb{Z}$; $\delta_{x,y}$ is the Kronecker symbol.

The functions $p(x)$ and $q(x)$ determine the probabilities to find a walker at the points $x-1$ and $x+1$, if it was at x at a previous moment of time, respectively; $r(x)$ corresponds to the probability of the adhesion (adsorption) [4]. In general, $p(x)$ and $q(x)$ are regarded as arbitrary non-negative functions less than $1/2$.

Let the sequence $\{a_n\}$ of N positive numbers,

$$0 = a_0 < a_1 < ... < a_{N-1} < a_N = \infty, \quad (2)$$

define the separation points of environment zones in space $x \in \mathbb{Z}_+$.

Reproducing the same configuration for negative x by inverting $a_n \to -a_n$, we introduce the characteristic functions χ_n of zones $[-a_n; -a_{n-1}] \cup [a_{n-1}; a_n]$: $\chi_n(x) = 1$ for $|x| \in (a_{n-1}; a_n)$, $\chi_n(\pm a_n) = \chi_n(\pm a_{n-1}) = 1/2$ to obtain always the arithmetic mean of the left- and right-handed functions at the separation points, and $\chi_n(x) = 0$ otherwise. To make use these in differential calculus, $\chi_n(x)$ are written as the distributions:

$$\begin{aligned}\chi_1(x) &= \theta(a_1 - |x|),\\ \chi_n(x) &= \theta(a_n - |x|) - \theta(a_{n-1} - |x|), \quad n > 1, \end{aligned} \quad (3)$$

where $\theta(x) = [1+\mathrm{sign}(x)]/2$ is the Heaviside function.

The functions $\{\chi_n\}$ are orthogonal:

$$\sum_{n=1}^{N} \chi_n(x) = 1, \quad |x| < a_N; \quad (4)$$

$$\chi_n(x)\chi_m(x) = 0 \quad \text{for} \quad n \neq m, \quad x \neq \{\pm a_n\}. \quad (5)$$

Given the basis, we further introduce $N+1$ constant parameters $\{d_n; V\}$, where $d_n \leq 1/2$ defines the diffusion coefficient for the n-th zone; V is a measure of probability asymmetry and plays the role of an external field. Supposing the drift velocity dependence

on the attractor strength and zone properties, we define the velocity in the n-th zone as $v_n = V\sqrt{d_n}$.

Thus, we consider the asymmetric RW in a heterogeneous environment with the following rules:

$$p(x) = \sum_{n=1}^{N} \left(d_n - \frac{1}{2} V \sqrt{d_n} \varepsilon_x \right) \chi_n(x),$$
$$q(x) = \sum_{n=1}^{N} \left(d_n + \frac{1}{2} V \sqrt{d_n} \varepsilon_x \right) \chi_n(x), \qquad (6)$$
$$r(x) = 1 - 2 \sum_{n=1}^{N} d_n \chi_n(x),$$

where $\varepsilon_x \equiv \mathrm{sign}(x)$.

To preserve the probability meaning of the functions $p(x)$ and $q(x)$, we require $0 < 2d_n \pm V\sqrt{d_n} \leq 1$.

The rules (6) allow us to simulate immediately the random trajectories for various sets $\{a_n; d_n; V\}$, which we analyze here analytically.

Physically, the definition of v_n leads to a common and finite time $\tau = 1/V^2$ of the advection residence in a whole space. Therefore, the n-th zone advection length $L_n^{\mathrm{a}} \simeq |v_n| t$ and the diffusion length $L_n^{\mathrm{d}} \simeq \sqrt{d_n t}$ give us the Peclet number [19] $\mathrm{Pe} \equiv (L_n^{\mathrm{a}}/L_n^{\mathrm{d}})^2 = t/\tau$ for all n. Thus, the both processes are tantamount at t obeying $\mathrm{Pe} \sim 1 \div 10$, as usual. At larger t, the advection becomes dominant.

Although we give a common analytical description at $V > 0$ and $V < 0$, these cases physically differ because of the repulsive or attractive role of the origin, where velocity sign is inverted due to ε_x. The scenario with $V < 0$ accords with the presence of a single attractor at $x = 0$, while the case of $V > 0$ admits the existence of two attractors at $x = \pm\infty$, which produce two particle flows moving in opposite directions.

The Markovian evolution of the probability distribution function (PDF) $P(x,t)$ such that $P(x,0) = \delta_{x,0}$ can be given by the master equation with arbitrary distances ℓ and times τ between successive steps as

$$P(x, t+\tau) = r(x)P(x,t) + p(x+\ell)P(x+\ell,t) + q(x-\ell)P(x-\ell,t). \qquad (7)$$

To obtain a differential equation at large t, (7) is expanded into the Taylor series up to the order $O(\ell^2, \tau)$. Omitting the rest terms, the lattice parameters are fixed to give constant scales $\ell/\tau = 1$ and $\ell^2/2\tau = 1/2$ of the drift velocity and diffusivity, respectively.

Further, defining the functions for all $d_n > 0$,

$$D(\alpha, x) = \sum_{n=1}^{N} (d_n)^\alpha \chi_n(x), \quad D(x) \equiv D(1, x), \qquad (8)$$

we arrive in the continuous limit at the differential equation for RW in the diffusion approximation:

$$\partial_t P(x,t) = \partial_x^2 [D(x)P(x,t)] - V\partial_x [\varepsilon_x D(1/2, x)P(x,t)], \qquad (9)$$
$$P(x,0) = \delta(x).$$

Differentiating, we can use $D'(\alpha+\beta, x) = D'(\alpha, x) \times D(\beta, x) + D(\alpha, x)D'(\beta, x)$, where the prime means the derivative with respect to a coordinate [1].

Note also that $D(\alpha, x)D(\beta, x) = D(\alpha+\beta, x)$ for $x \in \mathbb{R}\backslash\{\pm a_n\}$, and $D(\alpha, \pm a_n) \neq [D(\pm a_n)]^\alpha$ in general.

Evolving in space-time, the PDF defines the normalized statistical measure μ_t for a fixed t:

$$\mathrm{d}\mu_t = P(x,t)\mathrm{d}x, \quad \int \mathrm{d}\mu_t = 1, \qquad (10)$$

which is used for computing the averages.

3. Finding a PDF

To find a PDF, we follow [1] and concentrate the geometrical data in the new coordinate

$$\xi(x) = \int_0^x D(-1/2, x')\mathrm{d}x'. \qquad (11)$$

Note that the derivatives of $\xi(x)$ are singular, in general, at the points $x = \{\pm a_n\}$.

Integrating (11), we obtain $\xi(x) = \varepsilon_x X(-1/2, x)$,

$$X(\alpha, x) \equiv \frac{1}{2} \sum_{n=1}^{N} (d_n)^\alpha [l_n(x) - l_{n-1}(x)], \qquad (12)$$
$$l_n(x) = a_n - ||x| - a_n|.$$

We also define the functions $\tilde{D}(\alpha, \xi(x)) = D(\alpha, x)$:

$$\tilde{D}(\alpha, \xi) = \sum_{n=1}^{N} (d_n)^\alpha \tilde{\chi}_n(\xi), \qquad (13)$$

where $\tilde{\chi}_n(\xi) = \theta(b_n - |\xi|) - \theta(b_{n-1} - |\xi|)$, and $b_n \equiv \xi(a_n)$.

Then, introducing the probability distribution $\mathcal{P}(\xi,t)$, we re-write the statistical measure as

$$\mathrm{d}\mu_t = \mathcal{P}(\xi,t)\mathrm{d}\xi = \\ = \mathcal{P}(\xi(x),t)D(-1/2,x)\mathrm{d}x. \quad (14)$$

Substituting the re-defined $P(x,t)$ into (9), we arrive at the equation:

$$\partial_t\mathcal{P} + V\partial_\xi(\varepsilon_\xi\mathcal{P}) - \partial_\xi^2\mathcal{P} = \kappa\partial_\xi(\beta\mathcal{P}), \quad (15)$$

where the constant κ controls the interface effect between zones; $\mathcal{P}(\xi,0)=\delta(\xi)$.

Reformulating the model in terms of ξ, V is regarded as a global velocity, which takes the opposite signs in two infinite intervals of ξ: $\xi>0$ and $\xi<0$.

The right-hand side of (15) can be reduced to the form with $\beta(\xi)=\tilde{D}(-1/2,\xi)\partial_\xi\tilde{D}(1/2,\xi)$ and $\kappa=1$. The computations lead to the expression:

$$\beta(\xi) = \varepsilon_\xi\sum_{n=1}^{N-1}\beta_n\delta(|\xi|-b_n), \quad \beta_n = \frac{d_{n+1}-d_n}{2\sqrt{d_nd_{n+1}}}. \quad (16)$$

A sign of β_n is defined by the difference $d_{n+1}-d_n$, although the form of β_n can vary.

We substitute now a formal series in κ:

$$\mathcal{P}(\xi,t) = \varphi(\xi,t) + \sum_{r=1}^{\infty}\kappa^r\mathcal{S}_r(\xi,t), \quad (17)$$

where

$$\varphi(\xi,t) = \frac{1}{\sqrt{4\pi t}}\exp\left(-\frac{(|\xi|-Vt)^2}{4t}\right) - \\ - \frac{V}{4}\mathrm{e}^{V|\xi|}\mathrm{erfc}\left(\frac{|\xi|+Vt}{2\sqrt{t}}\right) \quad (18)$$

is a basic normalized solution to (15) at $\kappa=0$.

It is instructive to compare the fundamental solution $\theta(t)\varphi(\xi,t)$ with analytical solutions to the advection-diffusion equation under other conditions from the recent works [20–22].

The remaining problem is to examine the surface effect induced by $\beta(\xi)$, which disappears in the homogeneous environment.

In general, each term $\mathcal{S}_r$ is determined by the divergence $\partial_\xi(\beta\mathcal{S}_{r-1})$ with a point-like carrier on the right-hand side of (15) and, therefore, results in

$$\int_0^\infty \mathcal{S}_r(\xi,t)\mathrm{d}\xi = 0, \quad r\geq 1, \quad (19)$$

what preserves the normalization. This integral statistically means that $\mathcal{S}_r$ is a fluctuating sign-alternating function of space. Its magnitude is not suppressed by the factor κ^r, and the probability may fall down to negative values. Although series (17) allows us to calculate all of $\mathcal{S}_r$ in a simple way, the appropriate resummation is still needed.

Nevertheless, we compute here the first-order term $\mathcal{S}_1$ from the inhomogeneous equation

$$\partial_t\mathcal{S}_1 + V\partial_\xi(\varepsilon_\xi\mathcal{S}_1) - \partial_\xi^2\mathcal{S}_1 = \partial_\xi(\beta\varphi), \quad (20)$$

contracting $\varphi(\xi,t)$ with $\partial_\xi(\beta\varphi)$ to obtain

$$\mathcal{S}_1(\xi,t) = \sum_{n=1}^{N-1}\sum_{\epsilon=\pm}\epsilon\beta_n\mathrm{sign}(\xi-\epsilon b_n)I_n^\epsilon(\xi,t), \quad (21)$$

$$I_n^\pm(\xi,t) = \int_0^t f(\xi\mp b_n, t-\tau)\varphi(b_n,\tau)\mathrm{d}\tau, \quad (22)$$

where $f(\xi,t)=\partial_{|\xi|}\varphi(\xi,t)$; $b_n>0$.

Performing the integration, we get

$$I_n^\pm(\xi,t) = -\frac{1+V^2t}{4\sqrt{\pi t}}\exp\left(-\frac{(|\xi\mp b_n|+b_n-Vt)^2}{4t}\right) + \\ + \frac{V}{8}\mathrm{e}^{V(|\xi\mp b_n|+b_n)}\mathrm{erfc}\left(\frac{|\xi\mp b_n|+b_n+Vt}{2\sqrt{t}}\right)\times \\ \times[3+V(|\xi\mp b_n|+b_n)+V^2t]. \quad (23)$$

Limiting ourselves by accounting for the first-order correction, we obtain our main result for PDF:

$$P(x,t) = \varphi(\xi(x),t)D(-1/2,x) + \\ + \kappa\sum_{n=1}^{N-1}\beta_n[\mathrm{sign}(x-a_n)I_n^+(\xi(x),t) - \\ - \mathrm{sign}(x+a_n)I_n^-(\xi(x),t)]D(-1/2,x), \quad (24)$$

where $\mathrm{sign}(x\pm a_n)=\mathrm{sign}(\xi(x)\pm b_n)$.

At the vanishing V, this reproduces the result of [1] and describes the ordinary RW at $2d_n=1$ for all n, when $\xi(x)=\sqrt{2}x$ and $\beta_n=0$.

If $d_{n+1}=d_n$ for two neighboring zones, the interface points $x=\pm a_n$ become regular, and (24) welds these zones automatically.

Note that the correction by κ looks improper at $V<0$, because it has no static limit at large t, although the diffusion in the presence of an attractor at $x=0$ has to be a relaxation process leading to

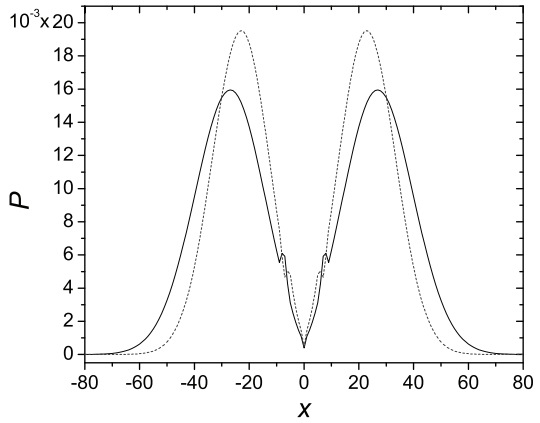

Fig. 1. Probability distribution function at $t = 200$ and $V = 0.2$ for two sets of environment parameters. Solid curve corresponds to the model with $2d_1 = 0.6$, $2d_2 = 0.4$, $2d_3 = 0.9$; the dashed one is for $2d_1 = 0.4$, $2d_2 = 0.9$, $2d_3 = 0.6$. In the both cases, $a_1 = 6$, $a_2 = 8$

a steady state distribution $P_{\rm eq}(x)$ and preventing a collapse $\langle x^2\rangle = 0$ due to the chaotic motion. Taking $t \to \infty$ and $\kappa = 0$ (or $\beta_n = 0$, equivalently) in (24), we obtain

$$P_{\rm eq}(x) = \frac{|V|}{2}\exp\left(-|V||\xi(x)|\right)D(-1/2, x). \tag{25}$$

This results in the limiting value of the variance $\langle x^2\rangle$ at $t \to \infty$, as we shall see. Thus, PDF (24) is applicable to the models with $V < 0$ at $\kappa = 0$.

Considering the case of $V > 0$, the surface term is relevant at $|\beta_n| \ll 1$, because $I_n^{\pm}$ is of the same order of magnitude as φ. As the result, Fig. 1 demonstrates two peaks of PDF, tending to escape in opposite directions to infinity with increasing t. However, the peak motion speeds for two sets of parameters look different because of different dampings caused by the adhesion.

Note finally that Eq. (15) can be transformed into the potential form by excluding the term $\partial_\xi \mathcal{P}$.

4. Probability Function

Using the PDF, let us compute the probability of the walker manifestation at a given space-time point,

$$\Pr(x,t) = \frac{1}{t}\int\limits_0^t P(x,\tau){\rm d}\tau, \tag{26}$$

that is the frequency of visiting a point x in a time t.

Integrating, $\varphi(\xi,t)$ results in

$$\Phi(\xi,t) = \frac{1}{\sqrt{4\pi t}}\exp\left(-\frac{(|\xi|-Vt)^2}{4t}\right)+$$
$$+\frac{1}{4Vt}\left[{\rm erfc}\left(\frac{|\xi|-Vt}{2\sqrt{t}}\right) - {\rm e}^{V|\xi|}{\rm erfc}\left(\frac{|\xi|+Vt}{2\sqrt{t}}\right)\right] -$$
$$-\frac{|\xi|+Vt}{4t}{\rm e}^{V|\xi|}{\rm erfc}\left(\frac{|\xi|+Vt}{2\sqrt{t}}\right). \tag{27}$$

Computing the total probability, we arrive at

$$\Pr(x,t) = \Phi(\xi(x),t)D(-1/2,x)+$$
$$+\kappa\sum_{n=1}^{N-1}\beta_n[{\rm sign}(x-a_n)\mathcal{I}_n^+(\xi(x),t)-$$
$$-{\rm sign}(x+a_n)\mathcal{I}_n^-(\xi(x),t)]D(-1/2,x), \tag{28}$$

where the first-order term in κ is determined by

$$\mathcal{I}_n^{\pm}(\xi,t) = \mathcal{I}(|\xi\mp b_n|+b_n,t), \tag{29}$$
$$\mathcal{I}(\xi,t) = -\frac{1}{\sqrt{4\pi t}}{\rm e}^{-(\xi-Vt)^2/(4t)}\left(1+\frac{V\xi+V^2t}{4}\right)+$$
$$+\frac{V}{4}{\rm e}^{V\xi}{\rm erfc}\left(\frac{\xi+Vt}{2\sqrt{t}}\right)\left[\frac{3}{2}+\frac{\xi}{Vt}+\frac{(\xi+Vt)^2}{4t}\right]. \tag{30}$$

We test our formulas by comparing $\Pr(x,t)$ with outcomes of numerical simulations. Data are presented in Fig. 2 and Fig. 3, putting $\kappa = 1$ and $\kappa = 0$, respectively, as it was argued above. Indeed, the bulk analytical solution is justified by the RW simulation in a three-zone environment. However, we hope for that the accounting for the series in κ or its finite part, at least, will allow us to reproduce better the considerable changes of the probability profile at short Δx.

The difference between peak heights obtained analytically and numerically at $x = 0$ is independent of the approximation in κ and can be also explained by the feature of our formalism describing mainly a walker behavior in bulk.

At $V < 0$, we see actually the coincidence of three probability functions inside zones: numerical one, $\Pr(x,t)$ at $t = 200$, and $\Pr_{\rm eq}(x) = P_{\rm eq}(x)$ at $t \to \infty$.

On the other hand, we observe a widening of the probability profile in Fig. 2 in comparison with one in [1] at $V = 0$ for the same environment parameters. Comparing, we also note the growing probability peaks in Fig. 2, *a*, which correspond to the

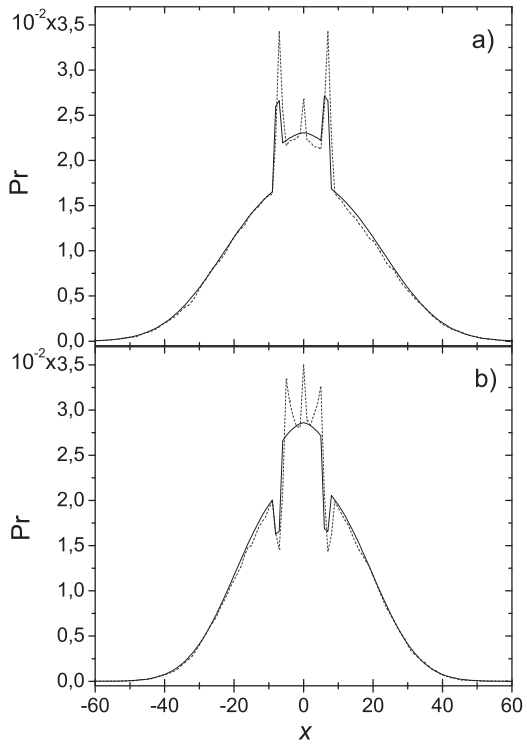

Fig. 2. Probability function at $t = 200$ and $V = 0.2$ for three-zone environment models. Solid lines are the analytical results given by (28). Dashed lines correspond to the numerical data of averaging over 3000 random trajectories. Panel (a): $2d_1 = 0.6$, $2d_2 = 0.4$, $2d_3 = 0.9$; (b): $2d_1 = 0.4$, $2d_2 = 0.9$, $2d_3 = 0.6$. In the both cases, $a_1 = 6$, $a_2 = 8$

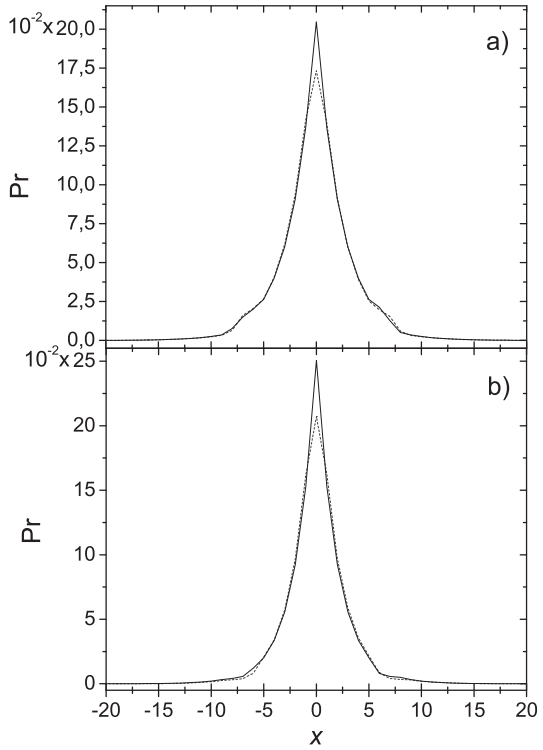

Fig. 3. Probability function at $t = 200$ and $V = -0.2$. Panels a, b correspond to the parameter sets in Fig. 2, respectively. Solid lines are analytically obtained; dashed ones represent the numerical results

zone with $2d_2 = 0.4$. It turns out that the presence of attractors causes the pumping effect, which depends on the local adsorption (determined by $r_n = 1-2d_n$) and is already revealed in the leading order ($\kappa = 0$).

5. Computing the Variance in the Leading Order

The variance $\langle x^2\rangle - \langle x\rangle^2$ is an important RW characteristic denoted here as

$$\Lambda(t) \equiv \int x^2 \mathrm{d}\mu_t; \quad \langle x\rangle \equiv \int x \mathrm{d}\mu_t = 0. \tag{31}$$

In our approach, we have $\Lambda(t) = \Lambda_0(t) + O(\kappa)$,

$$\Lambda_0(t) = \int\limits_{-\infty}^{\infty} [x(\xi)]^2 \varphi(\xi, t)\mathrm{d}\xi. \tag{32}$$

We focus on the properties of $\Lambda_0(t)$, corresponding to the leading-order approximation.

Although the function $x(\xi)$ can be presented similarly to (12), it is convenient to substitute it in terms of the characteristic functions $\{\tilde{\chi}_n(\xi)\}$. We find that

$$[x(\xi)]^2 = \xi^2 A_2(\xi) + |\xi| A_1(\xi) + A_0(\xi), \tag{33}$$

$$A_s(\xi) = \sum_{n=1}^{N} A_{s,n}\tilde{\chi}_n(\xi); \tag{34}$$

where the numerical coefficients are

$$A_{0,n} = \left(c_n - \sqrt{d_n} b_{n-1}\right)^2, \tag{35}$$

$$A_{1,n} = 2\left(\sqrt{d_n} c_n - d_n b_{n-1}\right), \tag{36}$$

$$A_{2,n} = d_n, \quad c_n = \sum_{m=1}^{n-1} \sqrt{d_m}\,(b_m - b_{m-1}). \tag{37}$$

Note that $A_2(\xi)$ coincides with the diffusivity $\tilde{D}(\xi)$.

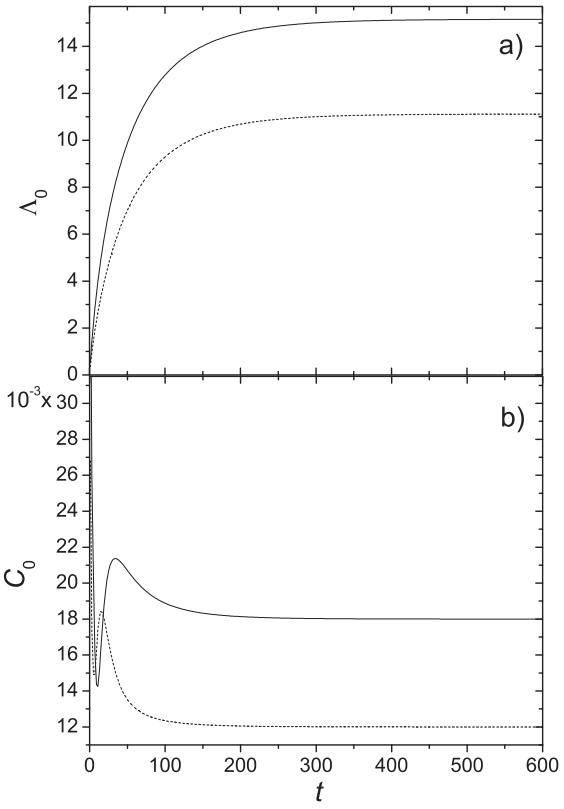

Fig. 4. Time dependences of the variance Λ_0 at $V=-0.2$ (a) and $C_0=\partial_t^2\Lambda_0/2$ at $V=0.2$ (b) for two sets of parameters. Solid curves correspond to $2d_1=0.6$, $2d_2=0.4$, $2d_3=0.9$; dashed ones are for $2d_1=0.4$, $2d_2=0.9$, $2d_3=0.6$

Combining the environment parameters $A_{s,n}$ and the time-dependent integrals, we write

$$\Lambda_0(t)=2\sum_{s=0}^{2}\sum_{n=1}^{N}A_{s,n}[U_{s,V}(b_n,t)-U_{s,V}(b_{n-1},t)], \quad (38)$$

where functions $U_{s,V}(b,t)$,

$$U_{0,V}(b,t)=\frac{1}{4}\mathrm{erf}\left(\frac{b-Vt}{2\sqrt{t}}\right)-\frac{\mathrm{e}^{Vb}}{4}\mathrm{erfc}\left(\frac{b+Vt}{2\sqrt{t}}\right), \quad (39)$$

$$U_{1,V}(b,t)=-\frac{1}{2}\sqrt{\frac{t}{\pi}}\exp\left(-\frac{(b-Vt)^2}{4t}\right)+$$
$$+\frac{1}{4V}\left[\mathrm{erf}\left(\frac{b-Vt}{2\sqrt{t}}\right)+\mathrm{e}^{Vb}\mathrm{erfc}\left(\frac{b+Vt}{2\sqrt{t}}\right)\right]+$$
$$+\frac{1}{4}\left[tV\mathrm{erf}\left(\frac{b-Vt}{2\sqrt{t}}\right)-b\mathrm{e}^{Vb}\mathrm{erfc}\left(\frac{b+Vt}{2\sqrt{t}}\right)\right], \quad (40)$$

$$U_{2,V}(b,t)=\left(t+\frac{V^2t^2}{4}-\frac{1}{2V^2}\right)\mathrm{erf}\left(\frac{b-Vt}{2\sqrt{t}}\right)-$$
$$-\frac{1}{2}\left(b+Vt+\frac{2}{V}\right)\sqrt{\frac{t}{\pi}}\exp\left(-\frac{(b-Vt)^2}{4t}\right)-$$
$$-\frac{2-2Vb+V^2b^2}{4V^2}\mathrm{e}^{Vb}\mathrm{erfc}\left(\frac{b+Vt}{2\sqrt{t}}\right), \quad (41)$$

determine the integrals for positive b (or $|b|$):

$$\int_0^b\xi^s\varphi(\xi,t)\mathrm{d}\xi=U_{s,V}(b,t)-U_{s,V}(0,t). \quad (42)$$

Questioning on the behavior of $\Lambda_0(t)$ at large t, the answers turn out to be sufficiently different for the models with $V<0$ and $V>0$, respectively. We can see that Fig. 4, a shows the existence of the equilibrium static limit $\langle x^2\rangle_{\mathrm{eq}}=\lim_{t\to\infty}\Lambda_0(t)$ at $V<0$, while Fig. 4, b indicates the ballistic regime for $V>0$ with $\langle x^2\rangle\sim C_0t^2$ at $t\to\infty$. Moreover, the environment structure given by the different sets of parameters $\{d_n\}$ does not affect these tendencies.

Assuming the presence of an attractor at $x=0$ ($V<0$) and taking $t\to\infty$ in (38), we have

$$\langle x^2\rangle_{\mathrm{eq}}=\frac{2d_1}{V^2}+\frac{1}{V^2}\sum_{n=1}^{N-1}\mathrm{e}^{-|V|b_n}\left[V^2(A_{0,n+1}-A_{0,n})+\right.$$
$$+|V|(A_{1,n+1}-A_{1,n})(1+|V|b_n)+$$
$$\left.+(d_{n+1}-d_n)\left(2+2|V|b_n+V^2b_n^2\right)\right]. \quad (43)$$

From whence, it follows that the maximum values of $\Lambda_0(t)$ for models in Fig. 4, a are $\langle x^2\rangle_{\mathrm{eq},1}\approx$ ≈ 15.16 and $\langle x^2\rangle_{\mathrm{eq},2}\approx 11.12$, when $(2d_1/V^2)_1=15$ and $(2d_1/V^2)_2=10$, respectively. Thus, the points $x=\pm\sqrt{\langle x^2\rangle_{\mathrm{eq}}}$ lie inside the first zone $(-a_1;a_1)$ for both models.

Focusing on the case of $V>0$, the time asymptotics of $\Lambda_0(t)$ is determined by the term containing $U_{2,V}(b_N,t)-U_{2,V}(b_{N-1},t)$ at $b_N\to\infty$. Thus, $\langle x^2\rangle=d_NV^2t^2$ at $t\to\infty$. This formula is valid, when the PDF peaks are far from the region $x\in$ $\in(-a_{N-1};a_{N-1})$ of the basic environment structure presence (see Fig. 1). Thus, we arrive at the asymptotic values of C_0 in Fig. 4, b: $(d_3V^2)_1=0.018$ and $(d_3V^2)_2=0.012$.

We would like to note that the velocity correlator $\tilde{C}=C_0-d_NV^2$ reproduces here the typical properties of C at $V=0$ from [1] for the same environment

parameters $\{a_n; d_n\}$. We observe the similarity in a sign-alternating $\tilde{C}$ at small t for the model with $2d_3 = 0.9$, while the regime $\tilde{C} > 0$ is preserved during the whole evolution for the model with $2d_3 = 0.6$.

Note that the sign of $\tilde{C}$ allows us to classify system's behavior. The stages with $\tilde{C} > 0$ correspond, as usual, to the superdiffusion. On the other hand, the regime with $\tilde{C} < 0$ reveals the transient subdiffusion caused by the particle capture for a short time by zones with relatively small d_n.

Thus, the adsorption effect of each zone determined by $r_n = 1 - 2d_n$ lasts to be important at $V > 0$, although a magnitude and time intervals of $\tilde{C}$'s variations depend on V. Moreover, the models with $V > 0$ give rise a possibility to investigate the influence of the distant zones in comparison with the models at $V = 0$ during the same time t. On contrary, the case of $V < 0$ does not allow us to overstep actually the first zone.

6. Discussion

We have considered an asymmetric RW model in a one-dimensional space densely covered by the finite-sized zones $x \in (-a_n, -a_{n-1}) \cup (a_{n-1}, a_n)$, $n = \overline{1, N}$, with the specified properties, which allows us to investigate the affect of inhomogeneities in different chaotic systems. Although the number of RW characteristics can be extracted from numerical simulations, the deeper analysis requires an analytical description, which would be based in the continuous limit on the advection-diffusion equation at the large total number of steps t associated with a time.

Our model initially formulated in terms of probabilities is designed also to include the familiar problems of RW with various barriers [2–8] into the concept of the heterogeneous environment. The present analysis is stimulated by the predictions and the unsolvable problems mentioned in those works.

Diffusion and advection are the main and competing processes, which we account for. Their parameters (diffusion coefficients $0 < d_n \leq 1/2$ and drift velocities $v_n = V\sqrt{d_n}$) varying from zone to zone allow us to reveal also the adsorption in bulk (determined by $r_n = 1 - 2d_n$) and the action of a long-range external field V. Sometimes, the latter notions are convenient for the physical treatment of observed phenomena.

We can also relate the diffusion coefficient to the effective walker mass $m_n = 1/2d_n$ in each zone. Then, from the point of view of a macroscopic particle ensemble, the mass variations might be interpreted as the result of a geometrically dependent interaction among particles, which is not specified here, but leads to the emergence of different states confined within zones.

Before summarizing the results, we note briefly the role of the advection which contributes to the directed motion of RW and is induced by a global asymmetry parameter $-1 < V < 1$ determining the preference between the left and right directions.

Precisely, the advection is involved here by means of the space-dependent velocity $\varepsilon_x V\sqrt{D(x)}$, where $\varepsilon_x \equiv \mathrm{sign}(x)$ makes the RW root point $x = 0$ to play the attractive or repulsive role depending on the sign of V. The case of $V < 0$ corresponds to the case where the point $x = 0$ attracts a walker. On contrary, at $V > 0$, we have a repulsor at $x = 0$, which pushes a walker away along one of the mutually opposite directions of axis x.

Technically, such a definition preserves the model symmetry under the coordinate inversion and leads to $\langle x \rangle = 0$ for any V.

Thus, under our assumptions, the probability to find a walker at a space-time point is determined by the diffusion and advection processes in various zones of the environment. Finding a probability distribution function from the advection-diffusion differential equation, the parameter constancy *almost* everywhere looks as a crucial condition of solvability of the problem. Indeed, the geometrical data are easily concentrated in a new spatial variable $\xi(x)$. It leads to an equation for the homogeneous environment with singular terms corresponding to the residual interface effects and containing the Dirac δ-function and its derivatives. Although this contradicts the probabilistic meaning of the quantities involved, it is a consequence of the use of distributions in the continuous limit. In the numerical simulations, no singularities are obtained. However, a receipt of obtaining a PDF by accounting for the interface contribution still has to be found. It may be resolved exactly by constructing the solutions with a gap [9], which is not considered here.

To obtain a PDF, we use a formal series in a switching parameter $\kappa \sim 1$, which controls the surface effects in the equation. The leading term by κ^0 gives us a basic normalized solution for the bulk, which is equal, in terms of ξ, to the fundamental solution

to the homogeneous system. Nevertheless, the resulting PDF of (x,t) reflects an environment complexity and the presence of the drift. We have also found a solution with the surface correction by κ^1, which is applicable at $V \geq 0$ and $|d_{n+1} - d_n| \ll 1$, as was shown above. We should use additional restrictions to limit the correction magnitude, which is not suppressed by κ.

Although such an approach is already exploited and justified by numerical simulations in [1] without drift, the inclusion of the advection changes considerably the dynamics of the system and the PDF form, which results in new outcomes.

We also compute the probability function in the linear approximation in κ and the variance dependence on t in the leading order, by neglecting the interface term.

For any N, we have revealed the time asymptotics of the variance:

$$\langle x^2 \rangle \sim t^{1+\mathrm{sign}(V)}, \quad t \to \infty. \tag{44}$$

This tendency is independent of the environment structure with $d_n > 0$, which is known to happen also for the uniform models.

However, the environment complexity leads to the effective power law $\langle x^2 \rangle \sim t^{\alpha}$ at finite t, with intermediate values of exponent α, indicating the transient anomalous diffusion. It is clearly seen at $V \geq 0$.

To show it, we appeal to the models with a three-zone environment given by the parameter sets from [1]. Furthermore, it is convenient to study the diffusion regimes by means of the velocity autocorrelation function

$$\tilde{C}(t) = \frac{1}{2}\frac{\mathrm{d}^2\langle x^2 \rangle}{\mathrm{d}t^2} - v_N^2, \quad v_N = V\sqrt{d_N}. \tag{45}$$

Then the super/sub-diffusion processes correspond to $\mathrm{sign}(\tilde{C}(t)) = 1/(-1)$, respectively. Using that, such time intervals are presented in Fig. 4, *b*.

It is worth to note that $\tilde{C}$ for a fixed set $\{a_n; d_n\}$ indicates a similar (anomalous) behavior at $V = 0.2$ and $V = 0$ (see [1]), although the possibility to observe an affect of distant zones at $V > 0$ is higher than at $V = 0$ for the same t.

Comparing the probability profiles at $V = 0.2$ and $V = 0$ (see [1]), we can see that the adsorption property of zones is intensified in the presence of the advection (see Fig. 2). Such a pumping effect looks surprisingly, because the advection and the diffusion are competing processes.

At negative values of V, we observe the PDF relaxation to a steady state distribution, as $t \to \infty$. Although a walker is attracted to the origin $x = 0$, the diffusion prevents a collapse with $\langle x^2 \rangle = 0$. However, there is no manifestation of all zones.

Note finally that the perspective subject of a forthcoming study is the analytical description of a model with independent local velocities $\{v_n\}$, by extending the parameter set up to $\{a_n; d_n; v_n\}$. The formalism accounting for local fluctuations $\delta\mathcal{D}(x) \equiv \mathcal{D}(x) - D(x)$ of the smoothly varied diffusivity $\mathcal{D}(x)$, where $D(x) = \sum_{\{n\}} d_n \chi_n(x)$, could be developed.

The authors are indebted for the partial support of this work by the Division of Physics and Astronomy of the NAS of Ukraine.

1. A.V. Nazarenko, V. Blavatska. A one-dimensional random walk in a multi-zone environment. *J. Phys. A: Math. Theor.* **50**, 185002 (2017).
2. M. Ascher. Explicit solutions of the one-dimensional heat equation for a composite wall. *Math. Comp.* **14**, 346 (1960).
3. G. Lehner. One-dimensional random walk with a partially reflecting barrier. *Ann. Math. Statist.* **34**, 405 (1963).
4. H.S. Gupta. Random walk in the presence of a multiple-function barrier. *J. Math. Sci. (Dehli)* **1**, 18 (1966).
5. J.E. Tanner. Transient diffusion in a system partitioned by permeable barriers. Application to NMR measurements with a pulsed field gradient. *J. Chem. Phys.* **69**, 1748 (1978).
6. O.E. Percus, J.K. Percus. One-dimensional random walk with phase transition. *SIAM J. Appl. Math.* **40**, 485 (1981); O.E. Percus. Phase transition in one-dimensional random walk with partially reflecting boundaries. *Adv. Appl. Prob.* **17**, 594 (1985).
7. P.S. Burada, P. Hänggi, F. Marchesoni, G. Schmid, P. Talkner. Diffusion in confined geometries. *Chem. Phys. Chem.* **10**, 45 (2009).
8. D.S. Novikov, E. Fieremans, J.H. Jensen, J.A. Helpern. Random walk with barriers. *Nat. Phys.* **7**, 508 (2011).
9. J.G. Powels, M.J.D. Mallett, G. Rickayzen, W.A.B. Evans. Exact analytic solutions for diffusion impeded by an infinite array of partially permeable barriers. *Proc. R. Soc. Lond. A* **436**, 391 (1992).
10. See, e.g., M.F. Shlesinger, B. West (ed.) *Random Walks and their Applications in the Physical and Biological Sciences* (AIP Conf. Proc., vol. 109) (AIP, 1984); F. Spitzer. *Principles of Random Walk* (Springer, 1976).
11. H.C. Berg. *Random Walks in Biology* (Princeton University Press, 1983).

12. E.A. Codling, M.J. Plank, S. Benhamou. Random walk models in biology. *J. R. Soc. Interface* **5**, 813 (2008).
13. A.R.A. Anderson, M.A.J. Chaplain, E.L. Newman, R.J.C. Steele, A.M. Thompson. Mathematical modelling of tumour invasion and metastasis. *J. Theor. Med.* **2**, 129 (2000).
14. S.C. Ferreira, jr., M.L. Martins, M.J. Vilela. Reaction-diffusion model for the growth of avascular tumor. *Phys. Rev. E* **65**, 021907 (2002).
15. P.J. Murray, C.M. Edwards, M.J. Tindall, P. K. Maini. From a discrete to a continuum model of cell dynamics in one dimension. *Phys. Rev.* E **80**, 031912 (2009).
16. M.J. Simpson, K.A. Landman, B.D. Hughes. Cell invasion with proliferation mechanisms motivated by time-lapse data. *Physica A* **389**, 3779 (2010).
17. S. Havlin, D. Ben Abraham. Diffusion in disordered media. *Phys. Adv.* **36**, 695 (1987).
18. R. Metzler, J.-H. Jeon, A.G. Cherstvy. Non-Brownian diffusion in lipid membranes: Experiments and simulations. *Acta BBA-Biomembr.* **1858**, 2451 (2016).
19. S.V. Patankar. *Numerical Heat Transfer and Fluid Flow* (McGraw-Hill, 1980).
20. J.S. Pérez Guerro, L.C.G. Pimentel, T.H. Skaggs, M.Th. van Genuchten. Analytical solution for the advection–dispersion transport equation in layered media. *Int. J. Heat Mass Trans.* **52**, 3297 (2009).
21. A. Kumar, D. Kumar Jaiswal, N. Kumar. Analytical solutions to one-dimensional advection–diffusion equation with variable coefficients in semi-infinite media. *J. Hydrol.* **380**, 330 (2010); A. Kumar, D. Kumar Jaiswal, R.R Yadav. Analytical solutions of one-dimensional temporally dependent advection-diffusion equation along longitudinal semi-infinite inhomogeneous porous domain for uniform flow. *IOSR J. Math.* **2**, 1 (2012).
22. R.N. Singh. Advection-diffusion equation models in near-surface geophysical and environmental sciences. *J. Ind. Geophys. Union* **17**, 117 (2013).

Received 15.04.17

А.В. Назаренко, В.Б. Блавацька

АСИМЕТРИЧНІ ХАОТИЧНІ БЛУКАННЯ В ОДНОВИМІРНОМУ БАГАТОЗОННОМУ СЕРЕДОВИЩІ

Р е з ю м е

Ми розглядаємо модель хаотичних блукань в одновимірному середовищі, сформованому кількома зонами скінченої ширини з фіксованими ймовірностями переходу. Також припускається, що переходи до лівої та правої сусідніх точок мають нерівні ймовірності. У неперервній границі, ми аналітично виводимо функцію розподілу ймовірності, яка, головним чином, визначається дифузією та дрейфом і пертурбативно враховує поверхневі ефекти між зонами. Вона використовується для обчислення ймовірності знаходження частинки у точці простору-часу та часової залежності середньоквадратичного відхилення частинки, яке виявляє перехідну аномальну дифузію. Для підтвердження нашого підходу, функція ймовірності порівнюється з результатами чисельного моделювання для тризонного середовища.